Research Report

**95-25**

# A Doubly Salient Permanent Magnet Motor Capable of Field Weakening

**Y. Li, T.A. Lipo**

Wisconsin Power Electronics Center
University of Wisconsin-Madison
Madison WI 53706-1691

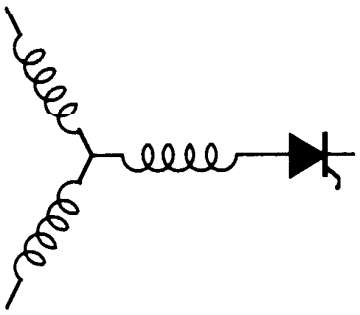

**W**isconsin
**E**lectric
**M**achines &
**P**ower
**E**lectronics
**C**onsortium

University of Wisconsin-Madison
College of Engineering
Wisconsin Power Electronics Center
*2559D Engineering Hall*
1415 Johnson Drive
Madison WI 53706-1691

# A DOUBLY SALIENT PERMANENT MAGNET MOTOR CAPABLE OF FIELD WEAKENING

Yue Li Thomas A. Lipo

Department of Electrical and Computer Engineering
University of Wisconsin - Madison
1415 Johnson Drive
Madison, WI 53706

**Abstract**—Permanent magnet (PM) machines have been used widely for industrial applications. However, the operating speed range in most of these applications is very limited due to the difficulty of achieving field weakening in most PM structures. This difficulty is one of the major stumbling blocks to widespread application of PM machines. A new doubly salient PM motor topology is proposed in this paper which offers the possibility of low cost, high performance and robust realization of field adjustment. It is shown that by controlling the field winding, 100% field weakening and 2 p.u. torque capability can be achieved without sacrificing other performance characteristics of the machine. Hence, machines of good efficiency throughout a field weakened speed range exceeding five to one can be readily devised This feature makes this new motor a potential candidate in future motor drive systems.

## I. Introduction

At present, there is an increasing tendency to consider machines with permanent magnet excitation for many applications because of their well-known high performance capability. However, as is well known, field control capability of PM machines is much more difficult to achieve than that with electric machines having wound field excitation. Also, the cost of high quality PM materials such as NdFeB PMs are still prohibitively high which limits the use of PM machines for many industrial applications. For the same reason, it has been difficult to employ PM motors in variable drive systems which require a wide operating speed range. In a high speed drive system, a field weakening capability is usually needed to obtain a wide constant power operatng range. To realize field weakening in PM machines a large number of ampere turns are usually required to overcome the large reluctance associated with interposing the PM in the main flux (magnetizing flux) axis of the machine which leads to a much higher overall cost of the system and poorer efficiency particularly during field weakening [1].

A new type of doubly salient PM motor capable of field weakening (FWDSPM) (see Fig. 1) is proposed in this paper which offers improved performance, high power density, low cost, field control capability and a robust structure for variable speed drives requiring a wide field weakening range. The doubly salient configuration of this machine provides higher flux concentration than sinusoidally distributed flux types and smoother torque production than other doubly salient PM structures due to the fact that the reluctance torque caused by self inductance variation vs. rotor angle can be greatly canceled [3-8]. On the other hand, sufficient room is arranged in this design for the use of ferrite PMs which are much less expensive than rare earth PMs. Moreover, because of this special arrangement, the PM reluctance seen by the field winding is fairly low so that the required ampere turns are comparatively small, sufficient to guarantee space for a wound field winding. In fact, PM machines having one hundred percent field weakening capability can be achieved by this method. Another advantage of this motor is that when the field winding is working in the field boosting mode, the starting torque capability can be as high as 2 p.u. and the output power of the machine can be increased by 30% at normal speed. The proof of this statement will be shown from the finite element analysis to be presented.

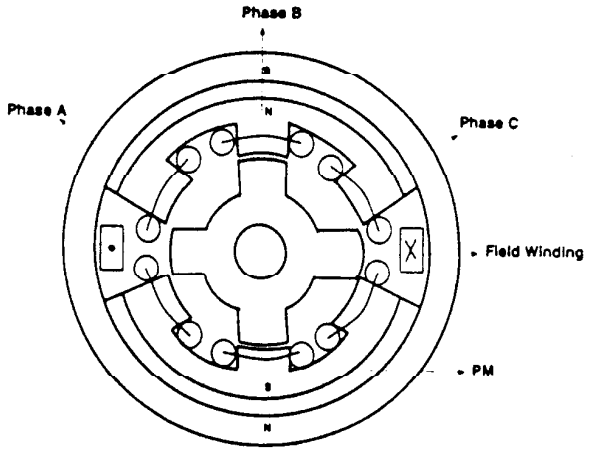


Fig. 1 Structure of the proposed FWDSPM motor.

## II. Operating Principle and Control Topologies

The operating principle of the FWDSPM motor is illustrated in Fig. 2. Due to the existence of PMs and the doubly salient structure of the machine, there are two kinds of torque produced in a FWDSPM motor: the PM torque (reaction torque), and the reluctance torque. The currents must be

controlled properly with the variation of phase PM flux linkage to obtain maximum PM torque which is normally the desired torque in this design as shown in Fig. 2. On the other hand, reluctance torque is also produced due to the saliency and is responsible for torque ripple at normal operating speed. To obtain smoother torque production, the reluctance torque should be controlled to be as small as possible. From a motor design point of view, both the magnitude and waveform of inductances must be carefully chosen in the design. In the proposed FWDSPM motor topology, part of the armature reaction flux will go through the magnets leading to a special self inductance waveform as illustrated in Fig. 2. The advantage of this waveform is the cancellation of the reluctance torque caused by self inductance variation, which guarantees less torque pulsation in this doubly salient structure. The magnitude of inductances can also be controlled by adjusting the field current. When field boosting mode is used (magnetizing field ampere turns), the iron of the motor will be highly saturated to limit the armature reaction flux. Based on this mechanism, torque ripple of this type of motor can be controlled without affecting the phase currents, which is a very important property of this design. As shown later, this property leads to 2 p.u. torque capability of this motor, an extremely desirable feature for traction applications.

One of the possible control topologies for FWDSPM motor is shown in Fig. 3. In this scheme, delta regulation is used in the current controller and a PWM rectifier is used as the field voltage controller. The tasks of the field voltage controller are:

i). To provide the proper ampere turns to boost or weaken the PM field. The behavior of the controller in this case is similar to a DC voltage source with polarity change capability.

ii). To assist current commutation and reduce torque ripple by controlling the saturation level of the motor. The behavior of the controller in this case is likened more to an AC voltage source with a DC component than a simple DC source.

As a result of the mutual coupling between the field winding and the armature windings, the variation of rotor angle will result in special AC current components in the field winding. Based on this mechanism, encoderless control could be realized in FWDSPM motors. More detailed results of encoderless control will be reported in another paper in the near future.

## III. Derivation of the Physical Model

The phase voltage equations of a three phase version of this machine can be expressed as follows:

$$\begin{bmatrix} ua \\ ub \\ uc \end{bmatrix} = \begin{bmatrix} ra & 0 & 0 \\ 0 & rb & 0 \\ 0 & 0 & rc \end{bmatrix} \begin{bmatrix} ia \\ ib \\ ic \end{bmatrix} + \begin{bmatrix} ema \\ emb \\ emc \end{bmatrix} + \frac{d}{dt} \begin{bmatrix} \lambda a \\ \lambda b \\ \lambda c \end{bmatrix} \qquad (1)$$

where $[e_{ma}, e_{mb}, e_{mc}]^t$ is the induced emf due to the magnet and the flux linkages and their time derivatives are,

$$\begin{bmatrix} \lambda a \\ \lambda b \\ \lambda c \end{bmatrix} = \begin{bmatrix} Laa & Mba & Mca \\ Mab & Lbb & Mcb \\ Mac & Mbc & Lcc \end{bmatrix} \begin{bmatrix} ia \\ ib \\ ic \end{bmatrix} = [L] \begin{bmatrix} ia \\ ib \\ ic \end{bmatrix} \qquad (2)$$

and

$$\frac{d}{dt} \begin{bmatrix} \lambda a \\ \lambda b \\ \lambda c \end{bmatrix} = [L] \begin{bmatrix} ia \\ ib \\ ic \end{bmatrix} + \left[ \frac{d[L]}{dt} \right] \begin{bmatrix} ia \\ ib \\ ic \end{bmatrix} \qquad (3)$$

So that

$$[ia \;\; ib \;\; ic] \begin{bmatrix} ua \\ ub \\ uc \end{bmatrix} = [ia \;\; ib \;\; ic][R] \begin{bmatrix} ia \\ ib \\ ic \end{bmatrix} + [ia \;\; ib \;\; ic] \begin{bmatrix} ema \\ emb \\ emc \end{bmatrix}$$
$$+ [ia \;\; ib \;\; ic][L] \begin{bmatrix} ia \\ ib \\ ic \end{bmatrix} + [ia \;\; ib \;\; ic] \left[ \frac{d[L]}{dt} \right] \begin{bmatrix} ia \\ ib \\ ic \end{bmatrix} \qquad (4)$$

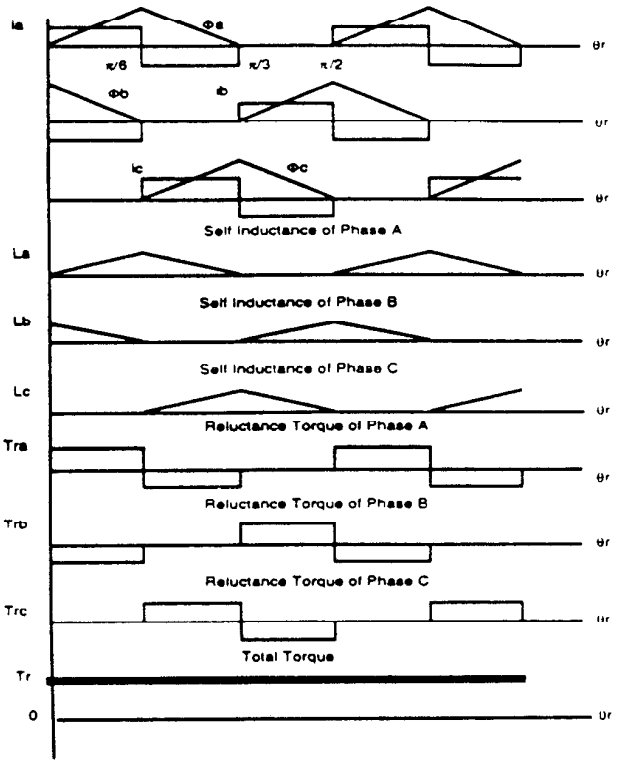


Fig. 2 Illustration of operating principle of FWDSPM motor. Variables from top to bottom: 1-3) current and magnet flux linkages of phases a-c respectively, 4-6) self inductance of phases a-c respectively, 7-9) reluctance torque of phases a-c respectively, 11) total torque (reaction plus reluctance torque)

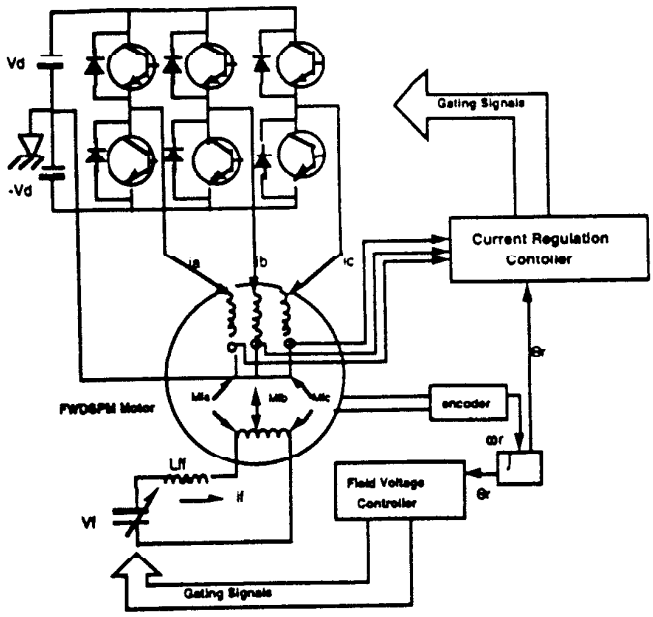


Fig. 3 Topology for speed control of FWDSPM motor.

Equation (4) can be interpreted as:

$$P_{in} = P_{cu} + T_m \times \omega_r + T_r \times \omega_r + \frac{d}{dt} W_f \qquad (5)$$

where

a) input power

$$P_{in} = \begin{bmatrix} ia & ib & ic \end{bmatrix} \begin{bmatrix} ua \\ ub \\ uc \end{bmatrix} \qquad (6)$$

b) copper loss

$$P_{cu} = \begin{bmatrix} ia & ib & ic \end{bmatrix} [R] \begin{bmatrix} ia \\ ib \\ ic \end{bmatrix} \qquad (7)$$

c) PM torque

$$T_m = \begin{bmatrix} ia & ib & ic \end{bmatrix} \begin{bmatrix} ema \\ emb \\ emc \end{bmatrix} \Big| \theta_r = \begin{bmatrix} ia & ib & ic \end{bmatrix} \begin{bmatrix} \frac{d\psi ma}{d\theta r} \\ \frac{d\psi mb}{d\theta r} \\ \frac{d\psi mc}{d\theta r} \end{bmatrix} \qquad (8)$$

d) reluctance torque

$$T_r = \frac{1}{2} \begin{bmatrix} ia & ib & ic \end{bmatrix} \begin{bmatrix} \frac{d[L]}{d\theta r} \end{bmatrix} \begin{bmatrix} ia \\ ib \\ ic \end{bmatrix} \qquad (9)$$

e) energy stored in armature windings

$$W_f = \frac{1}{2} \begin{bmatrix} ia & ib & ic \end{bmatrix} [L] \begin{bmatrix} ia \\ ib \\ ic \end{bmatrix} \qquad (10)$$

Also from (1), the dynamic equations of FWDSPM motor can be expressed by:

$$\frac{d}{dt} \begin{bmatrix} ia \\ ib \\ ic \end{bmatrix} = [L]^{-1} / [V] - [E] / - [L]^{-1} / [R] + \begin{bmatrix} \frac{d[L]}{d\theta r} \end{bmatrix} \omega r / \begin{bmatrix} ia \\ ib \\ ic \end{bmatrix} \qquad (11)$$

where

a) [V] is the control vector

$$[V] = \begin{bmatrix} ua \\ ub \\ uc \end{bmatrix} \qquad (12)$$

b) [E] is the PM voltage vector

$$[E] = \begin{bmatrix} ema \\ emb \\ emc \end{bmatrix} \qquad (13)$$

and c) [R] is the resistance matrix

$$[R] = \begin{bmatrix} ra & 0 & 0 \\ 0 & rb & 0 \\ 0 & 0 & rc \end{bmatrix} \qquad (14)$$

The machine parameters in (11) can be most readily obtained based on a finite element analysis (FEA) of the motor and digital computer simulations can be performed by using the dynamic equations derived herein. Furthermore, control strategies or the trajectory of vector [V] can also be studied based on this model. The PM voltage vector can be written as:

$$[E] = \begin{bmatrix} ema \\ emb \\ emc \end{bmatrix} = \begin{bmatrix} \frac{d\psi ma}{dt} \\ \frac{d\psi mb}{dt} \\ \frac{d\psi mc}{dt} \end{bmatrix} = \begin{bmatrix} \frac{d(\phi ma + Lmaif)}{dt} \\ \frac{d(\phi mb + Lmbif)}{dt} \\ \frac{d(\phi mc + Lmcif)}{dt} \end{bmatrix}$$

$$= \begin{bmatrix} \frac{d\phi ma}{dt} \\ \frac{d\phi mb}{dt} \\ \frac{d\phi ma}{dt} \end{bmatrix} + \begin{bmatrix} \frac{dLma}{dt} if \\ \frac{dLmb}{dt} if \\ \frac{dLmc}{dt} if \end{bmatrix} + \begin{bmatrix} Lma \frac{dif}{dt} \\ Lmb \frac{dif}{dt} \\ Lmc \frac{dif}{dt} \end{bmatrix} \qquad (15)$$

where

$\phi_{ma}$ - no load PM flux linked by phase A
$\phi_{mb}$ - no load PM flux linked by phase B
$\phi_{mc}$ - no load PM flux linked by phase C
$L_{ma}$- magnetizing inductance of the field winding for phase A
$L_{mb}$- magnetizing inductance of the field winding for phase B
$L_{mc}$- magnetizing inductance of the field winding for phase C
$i_f$ - field winding current

Usually the field current $i_f$ varies very slowly and the waveforms of $L_{ma}$, $L_{mb}$, $L_{mc}$ are the same as those of $\phi_{ma}$, $\phi_{mb}$, $\phi_{mc}$. Hence, equations (4-11) remain valid in spite of the fact that [E] is function of the field winding current. In this case $i_f$ can be considered simply as another control variable.

## IV. Finite Element Analysis of FWDSPM Motor

A finite element analysis for a 10 kW prototype FWDSPM motor has been completed to demonstrate the operating principle. The main task of this analysis was to obtain the necessary parameters for both designing and controlling the machine.

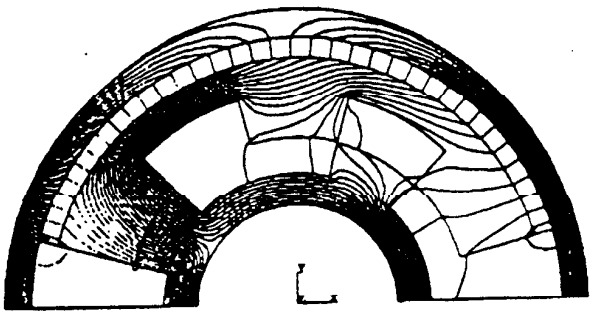

Fig. 4 Flux distribution of the prototype FWDSPM motor when only PM excitation exists.

Fig. 4 shows flux distribution when excited soley by PM excitation. It can be observed that a very high magnet flux concentration of ratio in the region of 4 to 1 in the active stator pole is achieved. Flux densities in the air gap on the order of 1.2 tesla can be readily obtained even though the working point within the ferrite magnet is only 0.3 tesla. This fact in turn, illustrates the flux focusing capability in a DSPM structure, far in excess of conventional buried PM machines.

Fig. 5 shows flux distribution when only armature current exists. The maximum inductance position is shown which occurs when the stator and rotor poles are half-overlapped. The special design the inductance profile as a function of rotor position leads to reduction of torque ripple as discussed previously.

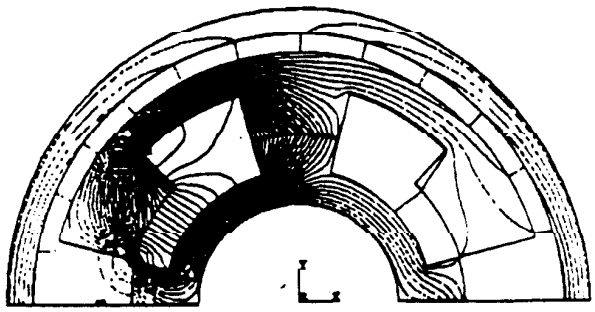

Fig. 5 Flux distribution of the prototype FWDSPM motor when only armature current excitation exists.

Fig. 6 shows phase PM flux linkage versus rotor angle under various levels of field current excitation. Note that very high field forcing is possible when the field current and magnet act to produce flux in the same direction. Conversely when the two fields oppose, the net flux in the gap can, if necessary, be driven to zero. The FEA indicates that the PM field can be fully canceled by the demagnetizing MMF provided by the field winding by using only 60~90% of the per unit field current (unity field current here is defined as the point where the volume current density of copper reaches 3,000 A/in$^2$).

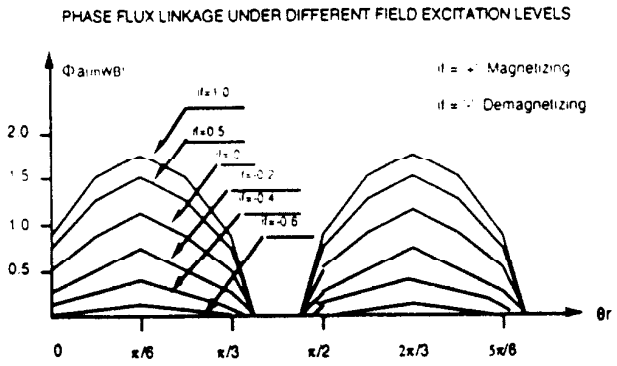


Fig. 6 Phase PM flux linkage versus rotor angle under different levels of field current excitations.

Based on the FEA study, the torque vs. speed characteristics of the motor can be determined as shown in Fig. 7. It can be noted that the starting torque capability of the motor can be as high as 2 p.u. when field boosting mode is used. In this case a highly saturated condition is achieved under this mode to greatly reduce the magnitude of inductances and thus the cogging torque.

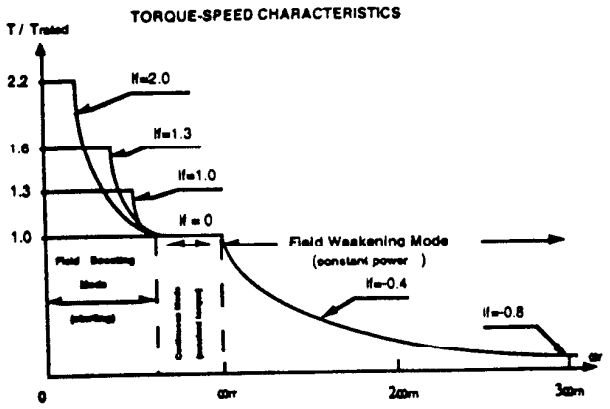


Fig. 7 Torque-speed characteristics of the FWDSPM motor under different field excitation levels

## V. Power Density Comparison with Induction Motor

Based on the above analyses, the power density of the FWDSPM motor can be obtained. Since the reluctance torque contributes no average torque to the torque production of the machine under normal operation condition, only the PM torque is considered for output power calculation. The derivation is given as follows:

The phase back-emf due to the variation of PM flux linkage can be expressed as,

$$E = \frac{P_s}{m} \times \frac{N_p \times \phi_m}{\theta_d} \omega_r \qquad (16)$$

where,

$P_s$ - stator pole number
$N_p$ - turn number per pole
$\phi_{pm}$ - peak PM flux linked by one pole coil (Wb)
$\omega_r$ - rotor speed (rad/sec)
$\theta_d$ - half period of PM flux variation (rad)
$m$ - phase number

and,

$$\theta_d = \frac{\pi}{P_s} \qquad (17)$$

$$\omega_r = \frac{2\pi \times n_s}{60} \qquad (18)$$

where

$n_s$ - mechanical speed (rpm)

From surface current density :

$$A = \frac{2N_p \times I_{rms} \times P_s}{\pi D_i} \qquad (19)$$

where

$D_i$ - stator inner diameter (M)

$I_{rms}$ - phase current rms value (A)

From (19), $N_p$ can be expressed as:

$$N_p = \frac{\pi D_i \times A}{2 I_{rms} \times P_s} \qquad (20)$$

The per pole PM flux is:

$$\phi_m = K_d \times \frac{\pi D_i}{2P_s} \times L_e \times B_g \qquad (21)$$

where

$K_d$ - PM flux leakage factor
$L_e$ - stack length (M)
$B_g$ - flux density in the air gap (Tesla)

From (16) - (21):

$$M \times E \times I_{rms} \times \eta = k_d \frac{\pi^2}{120} \eta \times B_g \times A \times n_s \times D_i^2 L_e \qquad (22)$$

where

$\eta$ - efficiency

Note that the output power of this motor is:

$$P_{out} = M \times E \times I_{avg} \times \eta = M \times E \times K_i \times I_{rms} \times \eta$$

where $I_{avg}$ is the average phase current and current factor $K_i$ is expressed as:

$$K_i = \frac{I_{avg}}{I_{rms}} \qquad (23)$$

Hence, the output equation of the FWDSPM motor can be obtained:

$$P_{out} = k_d \times K_i \frac{\pi^2}{120} \eta \times B_g \times A \times n_s \times D_i^2 L_e \qquad (24)$$

Comparing this result to the well known output equation of induction machine (IM), namely

$$P_{outIM} = \frac{\sqrt{2}\pi^2}{120} \eta \times \cos\phi \times n_s \times B_{g0} \times A \times D_i^2 L_e \qquad (25)$$

the power density ratio of the two machines can thus be obtained,

$$\xi = \frac{P_{outFWDSPM}}{P_{outIM}} = \frac{K_i}{\sqrt{2}} \frac{K_d}{\cos\phi_{IM}} \frac{B_g}{B_{g0}} \qquad (26)$$

Note that the constant $K_d$ for the FWDSPM motor is generally 0.8 - 0.9 which is about the same range as the power factor in an IM. The air gap flux density is the same as the tooth flux in a FWDSPM motor, so that it can be

as the tooth flux in a FWDSPM motor, so that it can be chosen as twice as that of the IM. Based on this analysis, the power density ratio can be further expressed as:

$$\xi = \frac{2K_i}{\sqrt{2}} \tag{27}$$

Due to the current waveform in the FWDSPM motor (shown in Fig. 2), if 60 electrical degrees is assumed in one stroke to correspond to the current commutation time, $K_i$ is calculated to be:

$$K_i = \frac{5}{\sqrt{42}} \tag{28}$$

So that

$$\xi = \frac{5}{\sqrt{21}} = 1.09 \tag{29}$$

From the derivation, a 9% power density increase is achieved without the help of the field winding. Also, recall that the stator surface current densities for the two motors were assumed the same. However, the current density of FWDSPM motor can be greater than the IM since a FWDSPM motor does not require rotor current. In reality, higher power density can be achieved in the FWDSPM motor by using the field boosting mode. Assuming that a one p.u. field current is used, from the FEA the per pole flux linkage could be increased by 50%, which suggests that the resultant PM torque can be increased by 50%. The performance of this machine can now be verified as below:

The additional copper loss due to the excitation of the field current is:

$$P_{cuf} = \rho \times J \times V_{cuf} \tag{30}$$

where,

$\rho$ - resistivity of copper
J - volume current density
$V_{cuf}$ - copper volume of the field winding

The volume $V_{cuf}$ in the proposed design is about 1.5 times of the copper volume of one phase armature winding $V_{cu}$. The armature winding copper loss can thus expressed by

$$P_{cu} = 3 \times \rho \times J \times V_{cu} \tag{31}$$

Hence,

$$P_{cuf} = \frac{1.5}{3} P_{cu} = \frac{1}{2} P_{cu} \tag{32}$$

From the above analysis, the output power is increased by 50% and the copper loss increased by 50%. If the iron loss is ignored, the efficiency of the motor will remain the same. However for a one p.u. field boosting mode, the power density ratio without sacrificinig good overall performance of the machine will be:

$$\xi = 1.5 \times 1.09 = 1.635 \tag{33}$$

## VI. Simulation Results

Digital simulations have been carried out for the design of a 3 phase 10 kw prototype FWDSPM motor. Machine data and performance calculation results are shown below:

| | | |
|---|---|---|
| Machine Data | | |
| stator outer diameter | 10.5 | inch |
| stator inner diameter | 6.0 | inch |
| stack length | 7.0 | inch |
| stator pole number | 6 | poles |
| rotor pole number | 4 | poles |
| stator/rotor pole arc | $30^0/30^0$ | |
| stator slot depth | 0.65 | inch |
| mechanical speed | 1800 | rpm |
| Machine Performance | | |
| DC bus voltage | 250 | volts |
| maximum inductance | 1.79 | mH |
| minimum inductance | 0.35 | mH |
| phase peak current | 100 | A |
| phase current RMS | 70.6 | A |
| output power | 10.6 | kw |
| efficiency | 96.5% | |

The simulation is based on the derived dynamic equations and the parameters obtained from the FEA. The current and voltage waveforms and torque production of the machine are shown in Fig. 8 and demonstrate the basic dynamic behavior of the machine. Of particular interest is the torque production of this machine which is composed of both PM and reluctance components. Note, in particular, that only a very small contribution to the overall torque is made by the reaction torquye. While this simulation was based on a finite element study, only several rotor positions were chosen to calculate inductances as function of current. Between any two adjacent positions, a linear relation was assumed to interpolate the values of inductances. A more accurate model of the motor is presently under development to simulate in detail the complete nonlinear behavior of the system

## VII. Conclusions

In this paper a doubly salient PM motor capable of field weakening has been proposed. It has been shown that this new PM machine topology combines the features of good performance, high torque capability, high flexibility for field adjustment, a robust structure and low cost. All of these advantages make this kind of machine a very competitive candidate for speed drive systems. A prototype machine is under construction and the experimental results will be reported shortly.

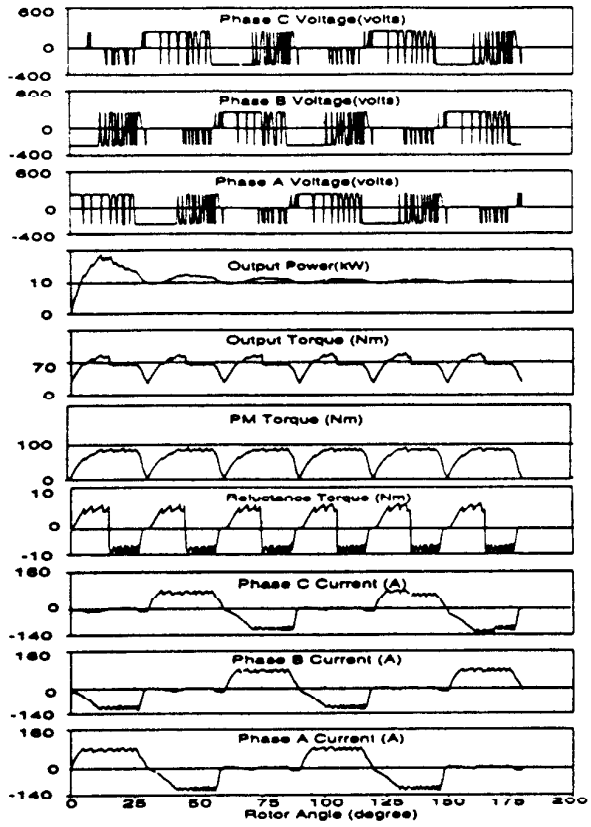


Fig. 8 Simulation results showing current waveforms for the prototype FWDSPM motor. Traces from the top: 1-3) Voltages of phases c, b and a respectively , 4) input power, 5) electromagnetic torque 6) reaction torque component 7) reluctance torque component, 8-10) Currents of phases c, b and a respectively, x- axis rotor angle in electrical degrees.

## References


[1] Pillay, P., (Editor),"Performance and Design of Permanent Magnet AC Motor Drives", Tutorial Course IEEE Ind. Appl. Society, Oct. 1-2, 1989.

[2] Lipo, T.A., Li, Y., "The CFM-A New Family of Electric Machines", *IPEC'95*, Yokohama Japan, April 1995, pp. 1-7.

[3] Li, Y., Leonardi, F., Lipo, T.A.,"A Novel Doubly Salient Permanent Magnet Generator Capable of Field Weakening", *DMMI* '95, Slovenia, May 17-19, 1995.

[4] Sarlioglu, B., Zhao, Y., and Lipo, T.A., "A Novel Doubly Salient Single Phase Permanent Magnet Generator ", *IEEE IAS* Annual Meeting, Denver CO, 1994, pp. 9-15.

[5] B. Sarlioglu and T. A. Lipo, "Comparison of Power Capability Between Doubly Salient Permanent Magnet and Variable Reluctance Type Generators" 1995 Agean Conference on Electrical Machines and Power Electronics, Kusadasi Turkey , (to appear).

[6] Liao, Y., Liang, F., and Lipo, T.A., "A Novel Permanent Magnet Motor with Doubly Salient Structure", *IEEE IAS* Annual Meeting, Houston TX, 1992, pp. 308-314.

[7] Liao, Y., "Design and Performance Evaluation of a New Class of Permanent Magnet Machines with Doubly Salient Structure", Ph.D Thesis, UW-Madison, 1992.

[8] Rauch, S.E. and Johnson, L.J., "Design Principles of Flux-Switch Alternators", *A.I.E.E. Trans. Dec* 1955, pp. 1261-1268.